Uncertainty estimates for the trilinear Higgs coupling at one-loop order in the Standard Model and its singlet extension

Jonas Scheibler, Technische Universität Dresden, Germany

Supervisors

Prof. Dr. Georg Weiglein, Dr. Johannes Braathen, Dr. Martin Gabelmann

DESY Theory Group, Hamburg

September 7, 2022

Abstract

This project investigates both, higher order- and parametric-uncertainties of the trilinear Higgs coupling λ_{hhh}. Concepts like *regularization* and *renormalization* are briefly explained and applied to the renormalization scheme conversion of Lagrangian parameters and subsequently λ_{hhh}. The parametric uncertainty is studied in both the Standard Model and one Beyond the Standard Model theory.

Contents

1 Introduction **3**

1.1 The Higgs sector in the Standard Model 3

1.2 The trilinear Higgs coupling λ_{hhh} 4

1.3 The study of λ_{hhh} with `anyBSM` 5

2 Higher order corections in quantum field theories **6**

2.1 Regularization and renormalization 6

2.2 Renormalization schemes 7

2.3 Renormalization scheme translation of λ_{hhh} 8

2.3.1 Renormalization of t_h 8

2.3.2 Renormalization of v 8

2.3.3 Results 9

3 parametric uncertainty of λ_{hhh} in the SM **9**

3.1 Preliminary investigations 9

3.2 parametric uncertainty estimates for λ_{hhh} 12

3.2.1 The "primitive" approach 12

3.2.2 The Gaussian and sum of squares approaches 12

3.2.3 Results 14

4 Parametric uncertainty of λ_{hhh} in the SSMZ2 **15**

4.1 The SSMZ2 BSM model 15

4.2 λ_{hhh} in the SSMZ2 model 15

4.3 Parameter uncertainties 16

4.4 results 18

5 Conclusions **19**

6 Acknowledgements **19**

1 Introduction

The Standard Model of particle physics (SM) governs our current description of fundamental interactions. With the exception of gravity, it is able to describe the fundamental particles and their interactions. Among these particles, the Higgs boson plays a special place. The study of the Higgs sector in the SM as well as in theories beyond the Standard Model (BSM) promises interesting new physics and solutions to problems of the SM. Current research in phenomenology emphasizes precision calculations as well as the investigation of specific parameters in the light experimental constrints.

1.1 The Higgs sector in the Standard Model

Consider only the kinetic and potential Higgs-terms for of the tree level SM Lagrangian

$$\mathcal{L} \supset (D_\mu \Phi)^\dagger (D^\mu \Phi) - V(\Phi)\,, \tag{1}$$

with

$$\Phi = \frac{1}{\sqrt{2}} \begin{pmatrix} \sqrt{2} G^+ \\ v + h + iG \end{pmatrix}, \qquad V^{(0)}(\Phi) = \mu^2 |\Phi|^2 + \lambda |\Phi|^4\,. \tag{2}$$

Tree level quantities are leading order terms in the pertubative expansion of a Lagrangian in a quantum field theory. The implications of higher order corrections are dicussed in chapter (2). The Higgs field is expanded around the minimum of the potential at its vacuum expectation value v: $\phi = \langle \phi \rangle + \delta\phi = v + h(x)$. Inserting Φ into $V(\Phi)$ and expanding, while disregarding terms involving G and G^+, we arrive at

$$\begin{aligned} V^{(0)} &\supset \frac{\mu^2}{2}(v+h)^2 + \frac{\lambda}{4}(v+h)^4 \\ &= \frac{\mu^2}{2}v^2 + \frac{\lambda}{4} + (\mu^2 v + \lambda v^3)h + (\frac{3}{2}\lambda v^2 + \frac{\mu^2}{2})h^2 + \lambda v h^3 + \frac{\lambda}{4}h^4\,. \end{aligned} \tag{3}$$

Introducing the new parameters t_h and m_h^2, the potential can be reparametrized into

$$t_h \equiv (\mu^2 + \lambda v^2)v\,, \qquad m_h^2 \equiv \mu^2 + 3\lambda v^2 \tag{4}$$

$$\implies V^{(0)} \supset t_h h + \frac{1}{2} m_h^2 h^2 + \frac{m_h^2 - \frac{t_h}{v}}{2v} h^3 + \frac{m_h^2 - \frac{t_h}{v}}{8v^2} h^4\,. \tag{5}$$

We use the derivatives of the reparametrized potential to define the quantities λ_{hhh} and λ_{hhhh} as

$$\lambda_{hhh} \equiv \left.\frac{\partial^3 V}{\partial h^3}\right|_{\text{min}}, \qquad \lambda_{hhhh} \equiv \left.\frac{\partial^4 V}{\partial h^4}\right|_{\text{min}}. \tag{6}$$

The minimalization condition of the potential can be expressed as

$$\left.\frac{\partial V^{(0)}}{\partial h}\right|_{\text{min}} \overset{!}{=} 0 = t_h\,. \tag{7}$$

Therefore we arrive at the tree level expression of λ_{hhh}

$$\lambda_{hhh} \equiv \left.\frac{\partial^3 V}{\partial h^3}\right|_{\min} = \frac{3(m_h^2 - t_h/v}{v} \, . \tag{8}$$

When investigating λ_{hhh}^{BSM} in BSM theories, usually the parameter κ_λ^{BSM} is introduced as

$$\kappa_\lambda^{BSM} = \frac{\lambda_{hhh}^{BSM}}{\lambda_{hhh}^{SM}} \, , \tag{9}$$

in order to quantify the deviation from the SM value.

1.2 The trilinear Higgs coupling λ_{hhh}

The trilinear Higgs coupling λ_{hhh} is an exceptionally interesting quantity for numerous reasons. In 2012, a SM-like Higgs particle was discovered at the CERN Large Hadron Collider (LHC) [1], proving also the existence of the Higgs potential. The measurement of the SM-like Higgs mass provided the electroweak minimum and the local curvature of said potential. However, the shape of the Higgs potential is also governed by λ_{hhh} and λ_{hhhh}. Investigations of these parameters could reveal answers to open questions about the electroweak phase transition in the early universe. Another reason for the study of λ_{hhh} is its sensitivity for BSM physics (eg. couplings to additional Higgs bosons). The SM implements a minimal Higgs sector, but an extended sector could provide a rich source for explanations of phenomena, like e.g. dark matter, that can't be explained within the SM.

The experimental study of λ_{hhh} via double Higgs production at hardon colliders is dominated by the two leading order processes, shown in figure (1). Figure (2) shows the cross section of the double Higgs production as a function of κ_λ^{BSM}. The theory prediction for κ_λ^{BSM} is currently constrained by experiment to a range of $-1 < \kappa_\lambda^{BSM} < 6$, provided that no other couplings do not significantly deviate from the SM prediction.

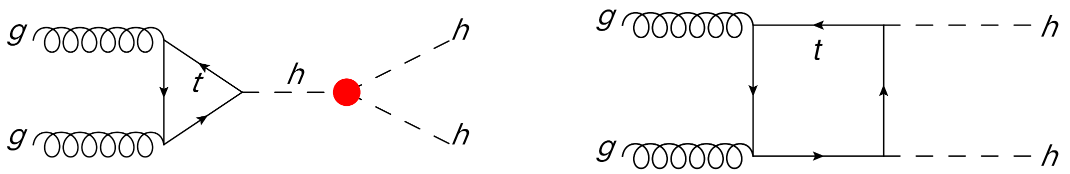

Figure 1: Leading order processes of two Higgs production

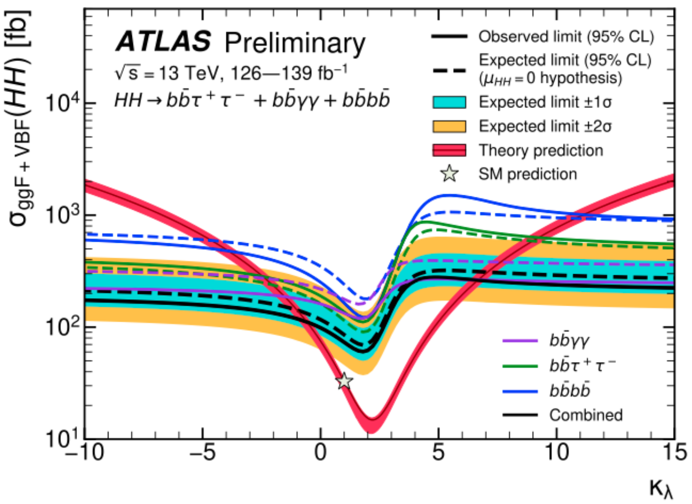

Figure 2: Total crossection for double Higgs production from the ATLAS collaboration.

1.3 The study of λ_{hhh} with `anyBSM`

The program `anyBSM`, developed by Henning Bahl, Johannes Braathen, Martin Gabelmann and Georg Weiglein provides the ability to calculate λ_{hhh} at one-loop (1L) order in the SM and BSM theories. In this project, `anyBSM` is used to estimate two-loop uncertainties on λ_{hhh} and calculate parametric uncertainties of λ_{hhh}, by taking into account experimental uncertainties for SM input parameters.

2 Higher order corections in quantum field theories

2.1 Regularization and renormalization

In an interacting quantum field theory (QFT), the parameters of the Lagrangian recieve higher order corrections. Divergences inevitably occur in the associated calculations and have to be treated in order to extract physically meaningful results. This delicate process can be divided into two major steps.
Regularization deals with the isolation of the divergencies. Multiple methods for several types of divergences exist, and in the following, an example of a common method of regularization, the so called dimensional regularization (DREG) will be shown. More detailed examinations on the topic can be found in [3], [4] and [5]. Consider the following one-loop integral, which is UV divergent.

$$A(x) = (16\pi^2)\int \frac{dk^4}{(2\pi)^4}\frac{1}{(k^2+x)} \tag{10}$$

The main step in the procedure is the modification of the spacetime dimension $4 \to d = 4 - 2\epsilon$ for the integration. The integration element changes accordingly

$$\frac{dk^4}{(2\pi)^4} \to \mu^{2\epsilon}\frac{dk^d}{(2\pi)^d} \tag{11}$$

In order to preserve the mass dimension of the intrgral, the parameter μ (regularization scale) has to be introduced. $A(x)$ can be evaluated as

$$\begin{aligned} A(x) &= (16\pi^2)\mu^{2\epsilon}\int \frac{dk^d}{(2\pi)^d}\frac{1}{(k^2+x)} = (16\pi^2)\frac{\pi^{d/2}\mu^{2\epsilon}\Gamma(1-\frac{d}{2})}{(2\pi)^d}x^{d/2-1} \\ &= x\left[-\frac{1}{\epsilon} + \gamma_E - \log(4\pi) - \log\big(\mu^2\big) + \log(x) - 1\right] \end{aligned} \tag{12}$$

Where γ_E is the Euler-Mascheroni constant. After the integration, the limit $\epsilon \to 0 \Leftrightarrow d \to 4$ has to be taken to return to four-dimensional spacetime. This limit reveals that the divergence has been separated into the $1/\epsilon$ pole.
Following the identification and isolation of the divergence, the process of *renormalization* removes the divergence from physical observables. As an example, we consider the propagator of a scalar field, which yields the following tree level result

$$S_h^{(0)} = \text{- - - - -} = i(p^2 - (m_h^0)^2)^{-1} \tag{13}$$

The higher order corrections can be considered in a particular way, namely by collecting all one particle irreducible (1PI) diagrams via a Dyson resummation, 1PI diagrams are the set of all diagrams that are not separable into two disconnected diagrams by cutting one internal line.

$$\begin{aligned} S_h(\not p) &= \text{- - - - -} + \text{- - - (1PI) - - -} + \text{- - - (1PI) - - (1PI) - - -} + \cdots \qquad (14a) \\ &= \frac{i}{p^2 - (m_h^2)_{ren} - \hat{\Sigma}_h(p^2)}\,. \qquad (14b) \end{aligned}$$

The term $\hat{\Sigma}$ appearing in the propagator in eq. (14) is the renormalized self energy of the particle. Beause $\Sigma(p^2)$ is a divergent quantity, one has to introduce a counterterm $\delta^{CT} m_h^2$. In this consideration, also a counterterm for scalar field δZ_ϕ appears.

$$\hat{\Sigma}(p^2) = \tag{15a}$$

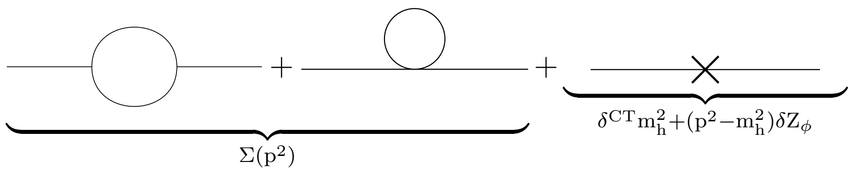

The physical mass (pole mass) of a particle is defined by the pole of the propagator (14). We define the pole mass M_h by the condition

$$p^2 - (m_h^2)_{ren} - \hat{\Sigma}_h(p^2) = 0 \tag{16}$$

$$\begin{aligned} \Longrightarrow \qquad M_h^2 &= (m_h^2)_{ren} + \hat{\Sigma}_h(p^2 = M_h^2) \\ &= (m_h^2)_{ren} + \hat{\Sigma}_h\{p^2 = (m_h^2)_{ren} + \hat{\Sigma}_h(M_h^2)\} \\ &= (m_h^2)_{ren} + \underbrace{\hat{\Sigma}_h(p^2 = (m_h^2)_{ren})}_{\mathrm{1L}} + \underbrace{\hat{\Sigma}_h(p^2 = M_h^2)\frac{\partial \hat{\Sigma}}{\partial p^2}(m_h^2)_{ren})}_{\mathcal{O}(\mathrm{2L})} \end{aligned} \tag{17}$$

Combining equations (15) and (17), we find

$$M_h^2 = (m_h^2)_{ren} + \hat{\Sigma}_h(p^2 = (m_h^2)_{ren}) = \Sigma_h(p^2 = (m_h^2)_{ren})|_{fin} + \delta^{CT} m_h^2|_{fin} \tag{18}$$

2.2 Renormalization schemes

In this project, two renormalization schemes were chosen, the on shell scheme (OS) and the modified minimal substraction scheme $\overline{\mathrm{MS}}$, which differ by the choice of the counterterm. The $\overline{\mathrm{MS}}$ scheme is designed to only cancel the divergent part

$$\delta^{CT,\overline{\mathrm{MS}}} m_h^2|_{fin} = 0 \tag{19}$$

In the OS scheme, the renormalized mass is set to be the physical mass, therefore

$$\delta^{CT,OS} m_h^2|_{fin} \stackrel{!}{=} -\Sigma_h(p^2 = (m_h^2)_{ren})|_{fin} \tag{20}$$

The counterterms are related, since both schemes treat the renormalization of the bare parameter $(m_h^0)^2$. Thus, we can translate between the schemes as follows

$$(m_h^0)^2 = (m_h^2)_{ren,\overline{\mathrm{MS}}} + \underbrace{\delta^{CT,\overline{\mathrm{MS}}} m_h^2}_{-\Sigma(\mathrm{p^2=(m_h^2)_{ren}})|_{\mathrm{div}}} = (m_h^2)_{ren,OS} + \underbrace{\delta^{CT,OS} m_h^2}_{-\Sigma(\mathrm{p^2=(m_h^2)_{ren}})|_{\mathrm{div+fin}}} \tag{21}$$

$$\Longrightarrow \ (m_h^2)_{ren,\overline{\mathrm{MS}}} = \underbrace{(m_h^2)_{ren,OS}}_{\mathrm{M_h^2}} - \underbrace{\Sigma(p^2 = (m_h^2)|_{fin}}_{\hat{\Sigma}(\mathrm{p^2=(m_h^2)_{ren}})|^{\overline{\mathrm{MS}}}} . \tag{22}$$

2.3 Renormalization scheme translation of λ_{hhh}

The following bare Lagrangian-quantities that contribute to λ_{hhh} recieve quantum corrections:

$$\begin{aligned} t_h^0 &\to t_h + \delta^{\text{CT}} t_h\,, \\ (m_h^2)^0 &\to m_h^2 + \delta^{\text{CT}} m_h^2\,, \\ v^0 &\to v + \delta^{\text{CT}} v\,, \\ h^0 &\to Z_h^{1/2} h = h\left(1 + \frac{1}{2}\delta^{\text{CT}} Z_h + \cdots\right)\,. \end{aligned} \tag{23}$$

The conversion of the (m_h^2) parameter has been discussed above. This chapter focuses on the renormalization of t_h and v.

2.3.1 Renormalization of t_h

The renormalization schemes of the so called tadpole parameter t_h can be translated analogously to (21), however further considerations have to be taken into account. The equation

$$t_h^0 = (t_h)_{ren,\overline{\text{MS}}} + \delta^{CT,\overline{\text{MS}}} t_h = (t_h)_{ren,OS} + \delta^{CT,OS} t_h \tag{24}$$

only holds if both schemes are evaluated either at the tree level, or the one-loop minimum of the Higgs potential V. The Fleischer-Jegerlehner scheme choses the tree level minimum of the potential, i.e. $t_h = 0$ and defines the $\overline{\text{MS}}$ counterterm to only cancel the divergent part of the one-loop contributions. This approach is the default treatment of the tadpole diagrams in `anyBSM`.

2.3.2 Renormalization of v

The vacuum expectation value v can be expressed in terms of the masses of the W- and Z-Boson, and the electric charge e in the following way

$$v = \frac{2M_W}{e}\sqrt{1 - \frac{M_W^2}{M_Z^2}} = \frac{2M_W}{\sqrt{\alpha_{QED}\pi}}\sqrt{1 - \frac{M_W^2}{M_Z^2}}\,. \tag{25}$$

Following the chain rule, the counterterm $\delta^{CT} v$ as a function of its parameters is

$$\frac{\delta^{CT} v}{v} = \sum_x \frac{\frac{\partial}{\partial X} v}{v} \delta^{CT} v\,, \qquad x = \{M_W, M_Z, e\} \tag{26}$$

The renormalization of M_W and M_Z is identical to (m_h^2). The renormalization of the electric charge e needs some further consideration.
In chapter (2.1), the self energy of a particle was introduced as a consequence of higher order corrections in in the propagator of a scalar particle. When considering gauge bosons (e.g. γ, W,Z), the Ward-Takahashi identity can be applied

$$p_\mu \Sigma_{VV'}^{\mu\nu} = 0 \implies \Sigma_{\gamma\gamma}^{\mu\nu}(p^2) = (p^2 g^{\mu\nu} - p^\mu p^\nu)\Pi_{VV'}(p^2)\,, \tag{27}$$

Following [2] (p.661 et seq.), we arrive at the expression for the counterterm δe of the electric charge

$$\frac{\delta e}{e} = \frac{1}{2}\Pi_{\gamma\gamma}(p^2=0)^{(1)} + \frac{\sin(\theta_w)}{\cos(\theta_w)}\frac{\Sigma^T_{\gamma Z}(p^2=0)}{M_Z^2}\,, VV' = \{\gamma\gamma, WW, ZZ, Z\gamma\} \tag{28}$$

The first term consists of the photon vacuum polarization, which contians contributions from heavy and light particles,

$$\Pi^{(1)}_{\gamma\gamma}(p^2=0) = \Pi^{(1)}_{\gamma\gamma}(p^2=0)\Big|_{\text{heavy}} + \underbrace{\Pi^{(1)}_{\gamma\gamma}(p^2=0)\Big|_{\text{light}}}_{\text{IR div.}}\,, \tag{29}$$

where the light-fermion contributions are IR-divergent at vanishing external momentum. The divergence can be cleverly avoided by introducing the quantity Δ_α, which is experimentally obtained,

$$\underbrace{\Pi^{(1)}_{\gamma\gamma}(p^2=0)\Big|_{\text{light}}}_{\text{IR div.}} = \underbrace{\Pi^{(1)}_{\gamma\gamma}(p^2=0)\Big|_{\text{light}} - \frac{\Sigma^{T,(1)}_{\gamma\gamma}(p^2=M_Z^2)}{M_Z^2}}_{\Delta_\alpha} + \underbrace{\frac{\Sigma^{T,(1)}_{\gamma\gamma}(p^2=M_Z^2)}{M_Z^2}}_{\text{not IR div.}} \tag{30}$$

2.3.3 Results

Following the chain rule analogously to (26), we arrive at the counterterm $\delta^{CT}\lambda_{hhh}$ of the trilinear coupling

$$\delta^{CT}\lambda_{hhh} = \frac{\partial\lambda^{(0)}_{hhh}}{\partial m_h^2}\delta^{CT}m_h^2 + \frac{\partial\lambda^{(0)}_{hhh}}{\partial t_h}\delta^{CT}t_h + \frac{\partial\lambda^{(0)}_{hhh}}{\partial v}\delta^{CT}v \tag{31}$$

The translation between the schemes is

$$\lambda^{(0)}_{hhh} = (\lambda_{hhh})_{ren,\overline{\text{MS}}} + \delta^{CT,\overline{\text{MS}}}\lambda_{hhh} = (\lambda_{hhh})_{ren,OS} + \delta^{CT,OS}\lambda_{hhh}\,. \tag{32}$$

Numerical results at one-loop order, obtained by `anyBSM`, for λ_{hhh} are

$$(\lambda_{hhh})_{ren,OS} = 176.758844804 \text{ GeV}, \tag{33}$$
$$(\lambda_{hhh})_{ren,\overline{\text{MS}}} = 180.406725994 \text{ GeV}. \tag{34}$$

Since both schemes have to be equal for infinite-loop order, the comparison of the results delivers an estimate for the higher order effects to be of the order of apprrox 3.65 GeV.

3 parametric uncertainty of λ_{hhh} in the SM

3.1 Preliminary investigations

Since λ_{hhh} is not known to infinite-loop order, uncertainty estimates play an important rule. In section (2.3.3), higher order contributions to λ_{hhh} were estimated. Another

source of uncertainty arises from the experimentally measured input-parameters of the SM (parametric uncertainty), which is investigated in this chapter.
Input-parameters entering λ_{hhh} at tree level can be read of equations (8) and (25). This consideration also investigates the top-quark mass parameter, which provides the main contribution at one-loop order. The values and associated uncertainties are provided by the Particle Data Group [6].

$$\begin{aligned} m_h^{pdg} &= (125.25 \pm 0.17)\ \mathrm{GeV} \\ m_Z^{pdg} &= (91.1876 \pm 0.0021)\ \mathrm{GeV} \\ m_W^{pdg} &= (80.377 \pm 0.012)\ \mathrm{GeV} \\ m_t^{pdg} &= (172.5 \pm 0.7)\ \mathrm{GeV} \\ \alpha^{pdg} &= 7.297352569311 \times 10^{-3} \pm 1.5 \times 10^{-10} \end{aligned} \tag{35}$$

In order to find the contributions from the parametric uncertainties on λ_{hhh}, the input parameters for these quantities were changed in the calculation in `anyBSM`. Figure 3 illustrates the parametric uncertainty. The numerical values are listed in table 2. The contribution of Δm_h is the largest, since m_h enters λ_{hhh} quadratically at tree level. Despite entering only at one-loop order, the contribution of Δm_t is half as large as that of Δm_h.

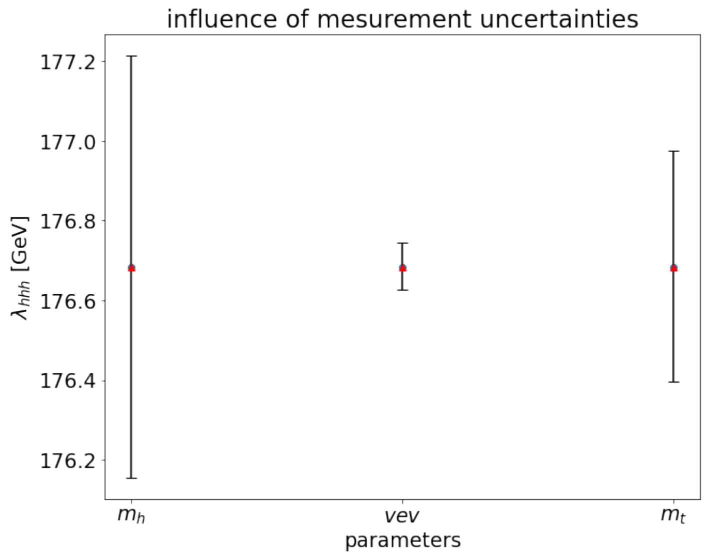

Figure 3: Influence of input parameters on λ_{hhh}

parameter	m_h	v	m_t
$\Delta\lambda_{hhh}$ / [GeV]	0.5302	0.0589	0.2903
$\Delta\lambda_{hhh}$ / [%]	0.3	0.0334	0.1643

Table 1: Numerical values of parametric uncertainties.

In order to investigate the parametric uncertainty of v, the respective, experimentally measured parameters in eq. (25) can be examined separately. Fig. 4 illustrates the assigned parametric uncertainties. The largest uncertainty, caused by Δm_W is below one order of magnitude smaller that the one caused by Δm_h. Since the experimental uncertainty of α^{pdg} is drastically smaller than that of the other parameters, the assigned parametric uncertainty is in any case negligible.

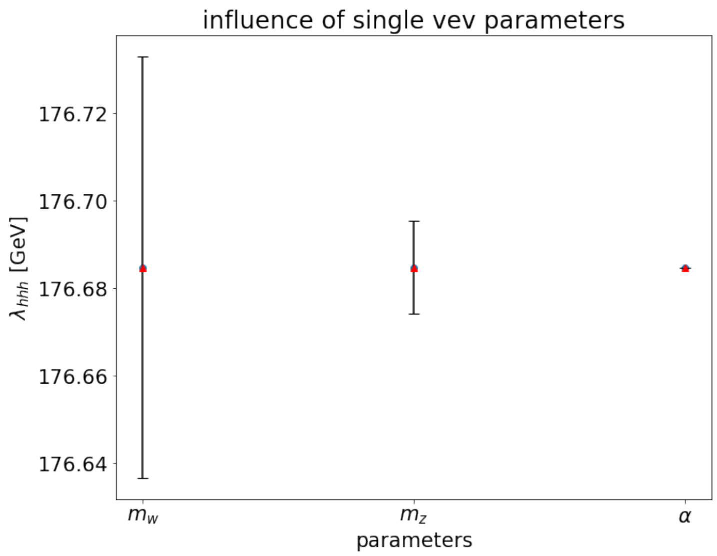

Figure 4: Influence of v input parameters on λ_{hhh}

parameter	m_W	m_Z	α
$\Delta\lambda_{hhh}$ / [GeV]	0.0483	0.0107	$1.475\ \times 10^{-6}$
$\Delta\lambda_{hhh}$ / [%]	0.027	0.006	$8.35\ \times 10^{-7}$

Table 2: Numerical values of parametric uncertainties in v.

3.2 parametric uncertainty estimates for λ_{hhh}

3.2.1 The "primitive" approach

In the previous section, the parametric uncertainties, caused by experimentally measured input parameters on λ_{hhh} have been investigated separately. In order to find a maximum value on the parametric uncertainty, simultaneous changes have to be included as well. In the so called "primitive" approach, the values of the input parameters have been varied only in terms of maximal or minimal estimates, e.g. $x \to x + \Delta x \quad \vee \quad x \to x - \Delta x$. A more sophisticated approach would be the proper minimalization/maximization of a multivariable function, however this was not pursued in this project. Table 3 shows the settings of the input parameters for minimalization and maximization of λ_{hhh} in the primitive approach.

parameter	m_h	m_W	m_Z	α	m_t
min	$m_h^{pdg} + \Delta m_h^{pdg}$	$m_W^{pdg} + \Delta m_W^{pdg}$	$m_Z^{pdg} - \Delta m_Z^{pdg}$	$\alpha^{pdg} + \Delta\alpha^{pdg}$	$m_t^{pdg}\Delta - m_t^{pdg}$
max	$m_h^{pdg} - \Delta m_h^{pdg}$	$m_W^{pdg} - \Delta m_W^{pdg}$	$m_Z^{pdg} + \Delta m_Z^{pdg}$	$\alpha^{pdg} - \Delta\alpha^{pdg}$	$m_t^{pdg}\Delta + m_t^{pdg}$

Table 3: Input parameters for minimalization- and maximization-case in the primitive approach.

3.2.2 The Gaussian and sum of squares approaches

Two well established methods in the field of error analysis, namely the sum of squares $(\Delta\lambda_{hhh})_S$ and Gaussian $(\Delta\lambda_{hhh})_G$ approach were also applied.

$$(\Delta\lambda_{hhh})_G = \left(\left(\left.\frac{\partial\lambda_{hhh}}{\partial m_h}\right|_{m_h^{pdg}} \right)^2 (\Delta m_h)^2 + \left(\left.\frac{\partial\lambda_{hhh}}{\partial m_W}\right|_{m_W^{pdg}} \right)^2 (\Delta m_W)^2 + \left(\left.\frac{\partial\lambda_{hhh}}{\partial m_h}\right|_{m_Z^{pdg}} \right)^2 (\Delta m_Z)^2 + \left(\left.\frac{\partial\lambda_{hhh}}{\partial \alpha}\right|_{\alpha^{pdg}} \right)^2 (\Delta \alpha)^2 + \left(\left.\frac{\partial\lambda_{hhh}}{\partial m_t}\right|_{m_t^{pdg}} \right)^2 (\Delta m_t)^2 \right)^{1/2} \tag{36}$$

$$(\Delta\lambda_{hhh})_S = \left((\Delta m_h)^2 + (\Delta m_W)^2 + (\Delta m_Z)^2 + (\Delta\alpha)^2 + (\Delta m_t)^2 \right)^{1/2} \tag{37}$$

Since `anyBSM` calculates λ_{hhh} at one-loop order, the derivatives in eq. (36) were calculated numerically using the method of central- and forward-differentiation. The choice of the values of these derivatives was made according to the plots shown in fig. 5.

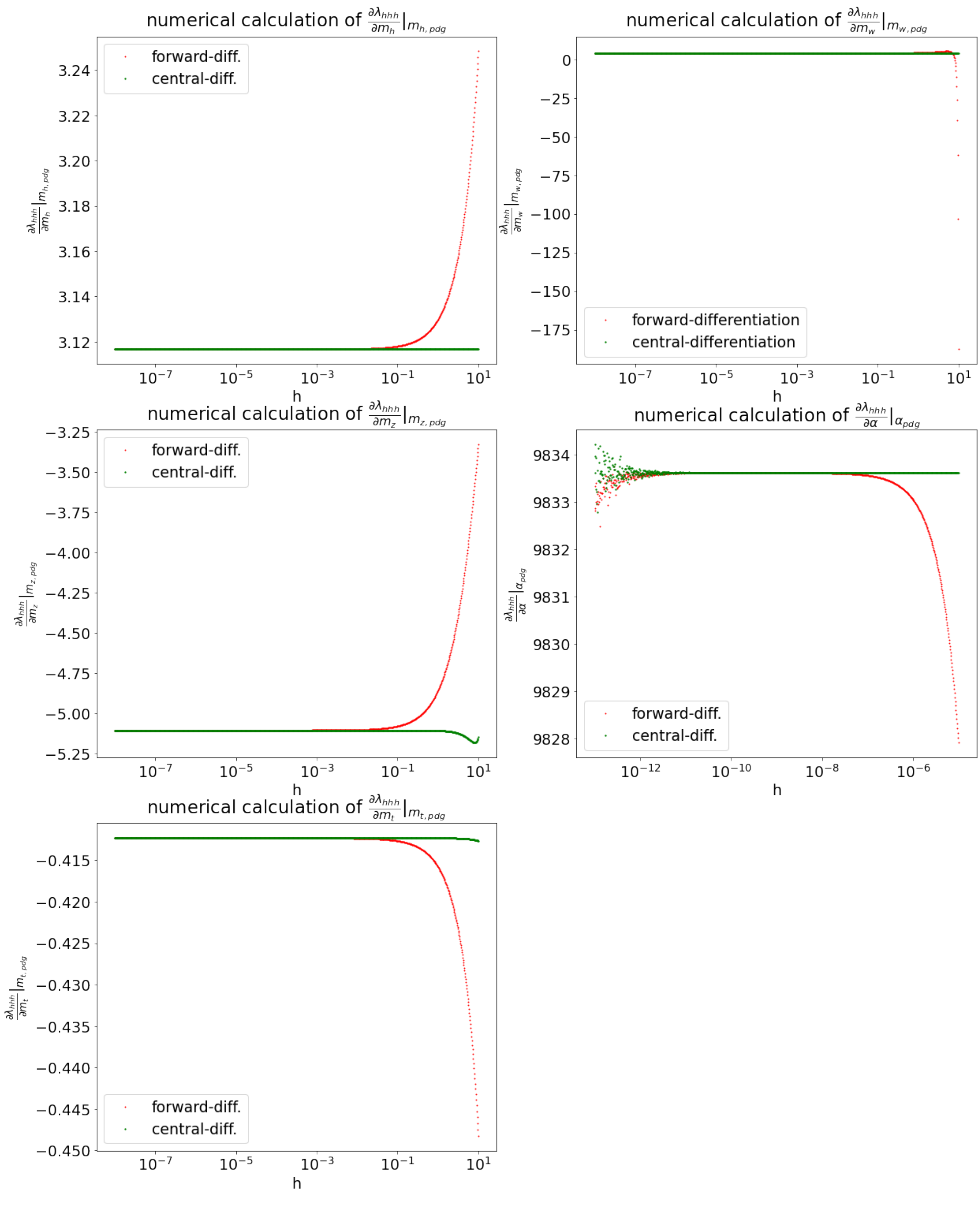

Figure 5: Numerical derivatives of λ_{hhh} with respect to the experimental parameters.

3.2.3 Results

The direct comparison of all estimates for the parametric uncertainty on λ_{hhh} is shown in fig. 6. Numerical results are illustrated in table 4. The primitive approach deliveres the largest error, followed by the sum of squares approach and the smallest estimate is provided by the Gaussian method.

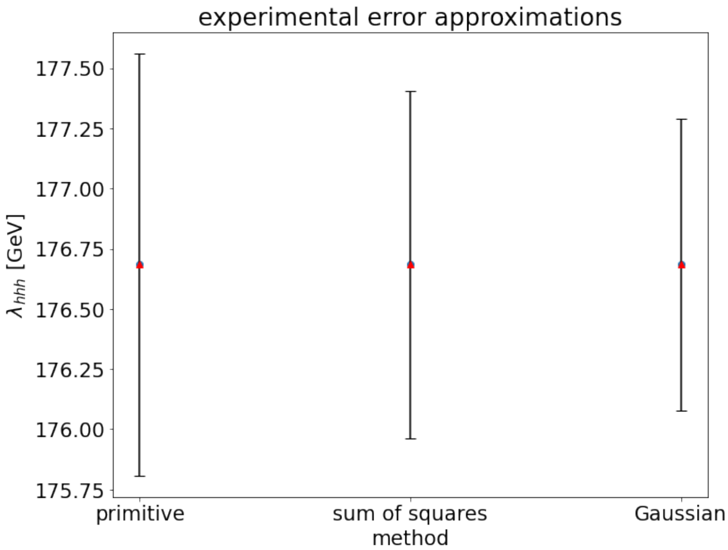

Figure 6: Parametric uncertainty of λ_{hhh} according to the applied approaches.

scheme	primitive	Gaussian	sum of squares
$\Delta\lambda_{hhh}$ / [GeV]	0.8779	0.7205	0.6054
$\Delta\lambda_{hhh}$ / [%]	0.497	0.408	0.343

Table 4: Numerical values of the parametric uncertainty estimates.

4 Parametric uncertainty of λ_{hhh} in the SSMZ2

4.1 The SSMZ2 BSM model

The SSMZ2 model describes a BSM model that includes an additional, real Singlet S, which introduces one new degree of freedom to the gauge sector. $\mathbb{Z}_2$ symmetry is imposed as an additional constraint, which means that the Lagrangian should not change under the transformation $S \to -S$. The scalar potential therefore only includes new terms involving even powers of S, it yields,

$$V(\phi, S) = \mu^2 \phi^\dagger \phi + \frac{\lambda}{2} |\phi^\dagger \phi|^2 + \frac{m_S^2}{2} S^2 + \frac{\lambda_S}{2} S^4 + \frac{\lambda_{SH}}{2} S^2 \phi^\dagger \phi \,. \tag{38}$$

The new terms involve new parameters m_S^2,which can be interpreted as a mass parameter for S, the quartic coupling λ_S and λ_{SH} which can be understood as a coupling between the SM-like Higgs doublett ϕ and the newly introduced singlet S. Because of the imposed $\mathbb{Z}_2$-symmetry, the tree level expression for λ_{hhh} remains the same as in the SM, but higher orders take corrections involving S into account and therefore λ_{hhh} should be sensitive to changes of m_S^2, λ_{SH} and λ_S.
The tree level mass of the Singlet is

$$M_S^2 = m_S^2 + \frac{\lambda_{SH}}{2} v^2 \,. \tag{39}$$

4.2 λ_{hhh} in the SSMZ2 model

As discussed above, a dependence of λ_{hhh} on the parameters[1] m_S^2 and λ_{SH} is to be expected. Fig. 7 depicts the impact of m_S^2 and λ_{SH} on λ_{hhh}.

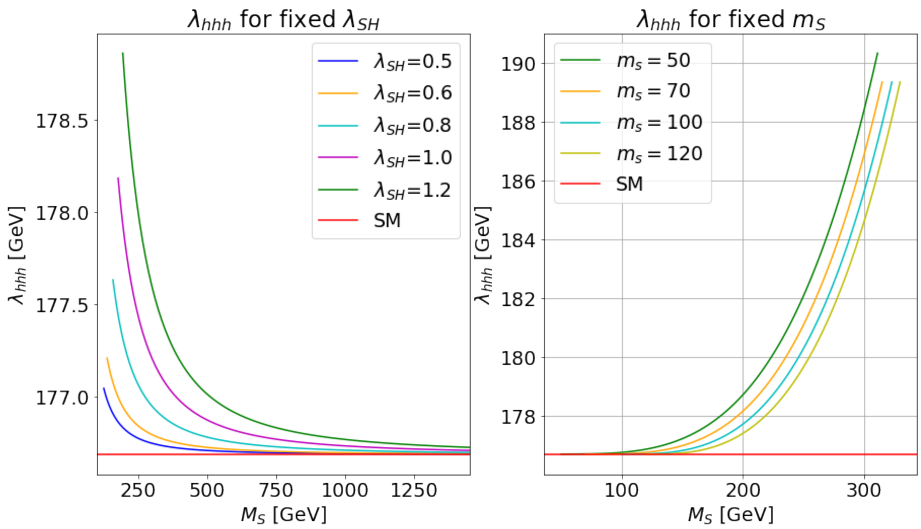

Figure 7: Impact of m_S^2 and λ_{SH} on λ_{hhh}.

[1]Corrections involving the quartic coupling λ_S enter at two-loop order.

Note, that all plots in fig. 7 converge converge into the SM prediction. M_S is calculated from eq. (39) for all cases. Small values of λ_{SH} convey small couplings and converge for large values of M_S (decoupling).

4.3 Parameter uncertainties

Analogously to the SM investigations, the parametric uncertainty of λ_{hhh} can be examined separately for all measured input-parameters (cf. eq. (39)). In this model, the dependence on m_S^2 and λ_{SH} is considered additionally.
Figures 8, 9 and 10 show the influence of the experimental uncertainties of the respective input parameters on λ_{hhh}. For all parameters, the errorbands converge into the SM prediction in the same way as in the Standard Model.

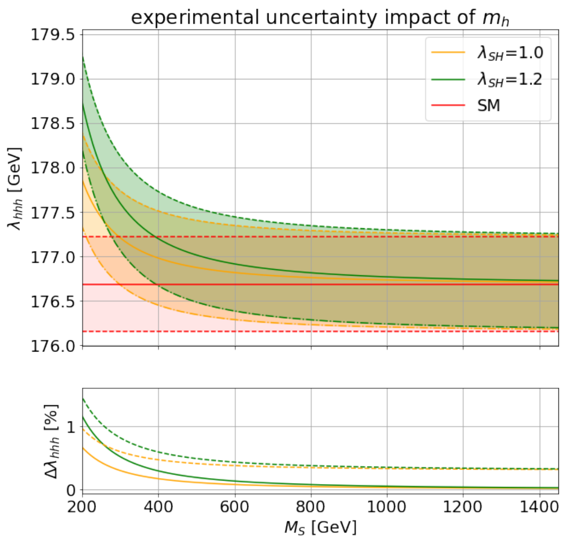

(a) Impact of the experimental m_h-uncertainty on λ_{hhh} for fixed λ_{SH}.

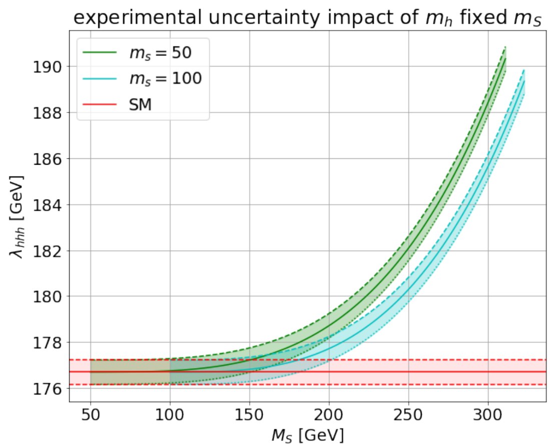

(b) Impact of the experimental m_h-uncertainty on λ_{hhh} for fixed m_S.

Figure 8: Parametric uncertainty of m_h.

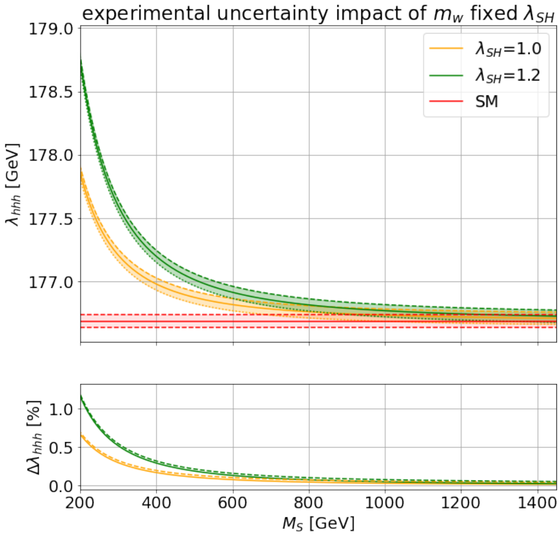

(a) Impact of the experimental m_w-uncertainty on λ_{hhh} for fixed λ_{SH}.

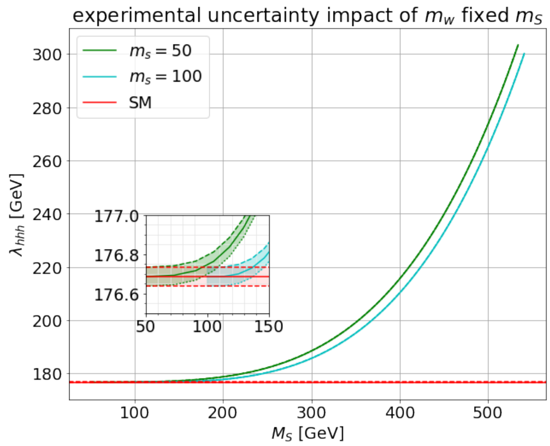

(b) Impact of the experimental m_w-uncertainty on λ_{hhh} for fixed m_S

Figure 9: Parametric uncertainty of m_W.

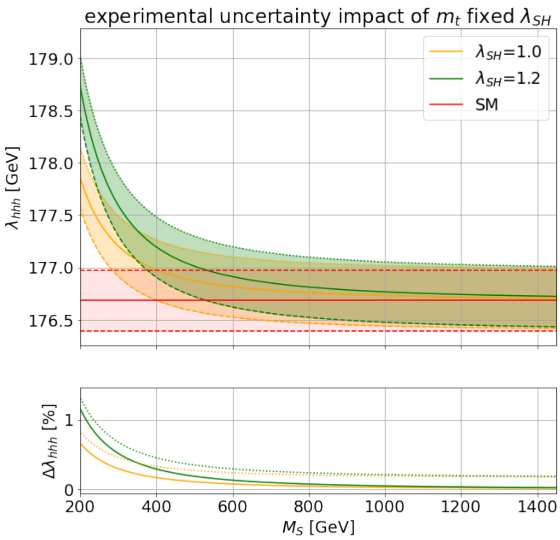

(a) Impact of the experimental m_t-uncertainty on λ_{hhh} for fixed λ_{SH}.

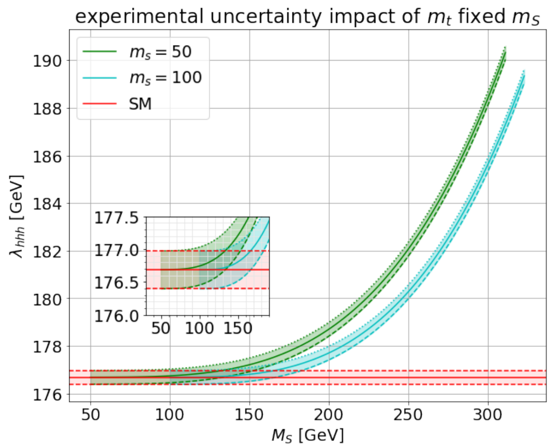

(b) Impact of the experimental m_t-uncertainty on λ_{hhh} for fixed m_S.

Figure 10: Parametric uncertainty of m_t.

4.4 results

In order to obtain proper uncertainty estimates, same methods as in sec. (3.2) can be applied to the SSMZ2 case. Figures (11) and (12) depict λ_{hhh} with the assigned errorbands for the respective estiamates. For both cases, fixed λ_{SH} or fixed m_S the errorband estimates converge into the SM case (cf. fig. 6).

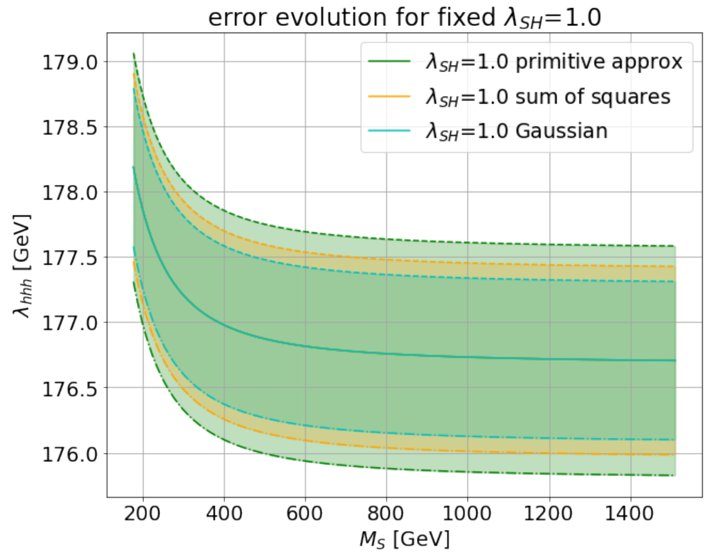

Figure 11: Parametric uncertainty of λ_{hhh} for fixed λ_{SH}.

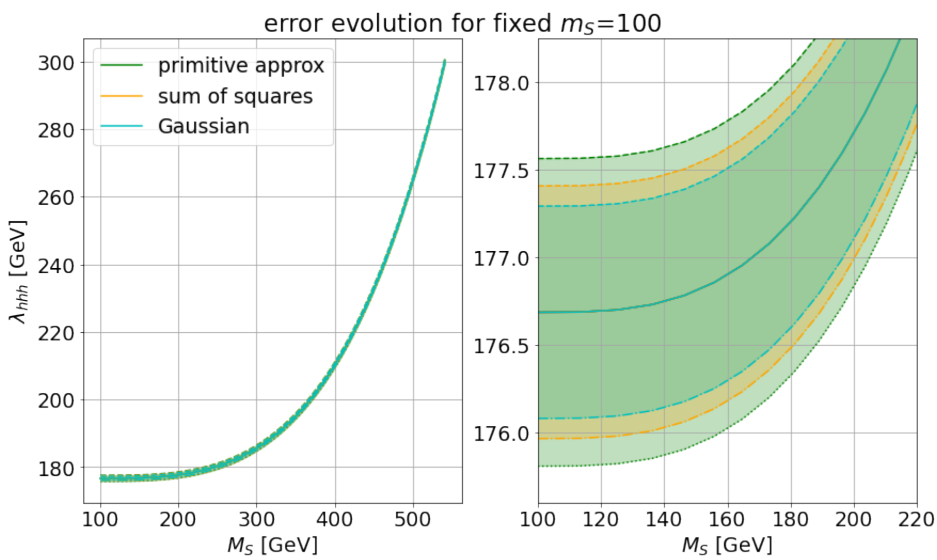

Figure 12: Parametric uncertainty of λ_{hhh} for fixed m_S.

5 Conclusions

In this project, `anyBSM` was applied in order to obtain both higher order- and parametric-uncertainties of the trilinear Higgs coupling λ_{hhh}. Especially for the renormalization scheme conversion, the concepts of renormalization and regularization were introduced and to some degree familiarized. The study of the parametric uncertainty was conducted not only in the SM but also in the SSMZ2 BSM model. The BSM considerations converged neatly into the SM case, showcasing advanced concepts like decoupling.

6 Acknowledgements

I thank my supervisors Johannes Braathen, Martin Gabelmann and Georg Weiglein for creating and conducting such an exciting internship. I am especially thankful to Johannes Braathen and Martin Gabelmann for devoting very generous ammounts of time and effort into explanations and discussions and therefore enabling me to take part in this research project. I am also thankful to Alain Verduras for many engaging discussions and a lot of fun memories of this project.
I also want to mention the DESY T group for the friendly and exciting work environment and the organizing team of the DESY Summer Student Program for the creation of this exciting program.

References

[1] G. Aad et al. "Observation of a new particle in the search for the Standard Model Higgs boson with the ATLAS detector at the LHC". In: *Physics Letters B* 716.1 (Sept. 2012), pp. 1–29. DOI: `10.1016/j.physletb.2012.08.020`. URL: `https://doi.org/10.1016%2Fj.physletb.2012.08.020`.

[2] M. Bohm, Ansgar Denner, and H. Joos. *Gauge theories of the strong and electroweak interaction*. 2001. ISBN: 978-3-519-23045-8, 978-3-322-80162-3, 978-3-322-80160-9. DOI: `10.1007/978-3-322-80160-9`.

[3] Johannes Braathen. "Automating Higgs precision calculations". PhD thesis. Paris, LPTHE, 2018.

[4] Martin Gabelmann. "Two-Loop Corrections to Higgs Boson Masses in the NMSSM". PhD thesis. Karlsruher Institut für Technologie, KIT, Karlsruhe, EKP, 2021.

[5] Marcel Krause. "On the Renormalization of the Two-Higgs-Doublet Model". MA thesis. KIT, Karlsruhe, TP, 2016.

[6] R. L. Workman et al. "Review of Particle Physics". In: *PTEP* 2022 (2022), p. 083C01. DOI: `10.1093/ptep/ptac097`.